

Resveratrol Glucosylation by GTF-SI from *Streptococcus mutans*: Computational Insights into a GH70 Family Enzyme

Electronic Supplementary Information

Camilo Febres-Molina,^a Xavier Prat-Resina^b and Gonzalo A. Jaña^{*c}

^a Doctorado en Físicoquímica Molecular, Facultad de Ciencias Exactas, Universidad Andres Bello, Santiago - Chile. ^b Center for Learning Innovation, University of Minnesota Rochester, Rochester, Minnesota 55904, United States. ^c Departamento de Ciencias Químicas, Facultad de Ciencias Exactas, Universidad Andres Bello, Concepción - Chile. E-mail: gonzalo.jana@unab.cl

*Author to whom correspondence should be addressed.
gonzalo.jana@unab.cl

Contents

Supplementary figures

1	Fig. SF1 Crystallographic structure of glucosyltransferase-SI	3
2	Fig. SF2 Active site residues RMSD for MD _{rest} and MD _{free} systems	4
3	Fig. SF3 RMSF represented by B-factor on both systems proteins.	5
4	Fig. SF4 Active site water molecules.	5
5	Fig. SF5 SASA histograms	6
6	Fig. SF6 Solvent-accessible volume on both systems proteins.	6
7	Fig. SF7 Arg ⁴⁷⁵ interaction.	7
8	Fig. SF8 Eigenvectors of the transition state frequency calculation.	8

Supplementary table

1	Table ST1 Activation barriers calculated at the QM(DFTB3)/MM of six GTF-SI MD _{rest} frames and the DFT-based structure	7
---	---	---

Supplementary Materials

The coordinates of the relevant states along the Minimum Energy Path for the study of Resveratrol Glucosylation by GTF-SI can be accessed at the following link: [GitHub Repository](#).

Supplementary Figures

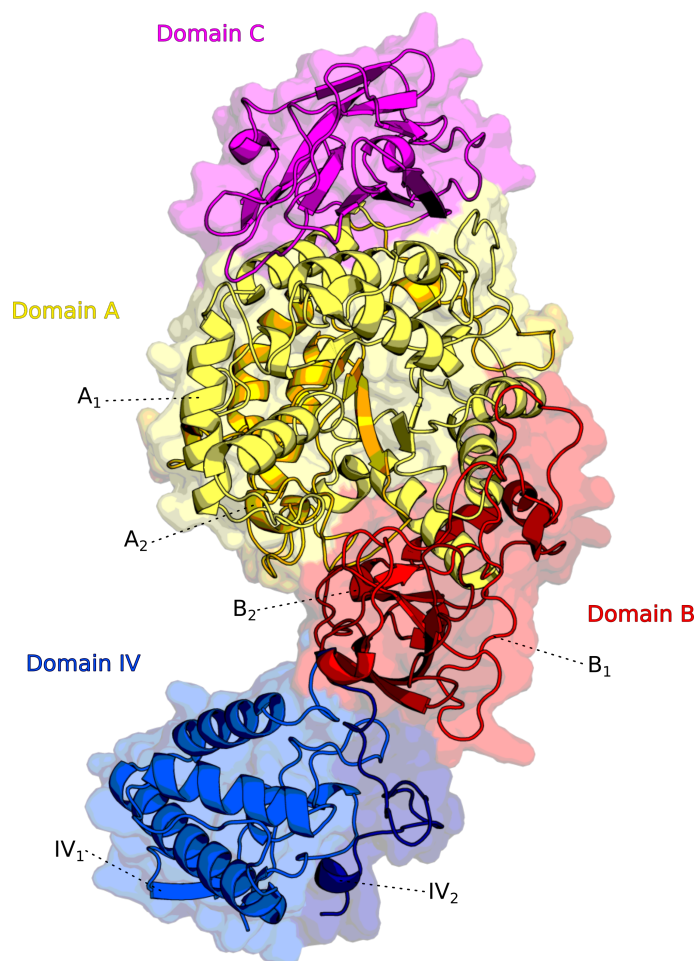


Fig. SF1 Crystallographic structure of glucosyltransferase-SI with PDB ID 3AIE - chain C.¹ Domains A, B, IV, and C are depicted in shades of yellow, red, blue, and magenta, respectively.

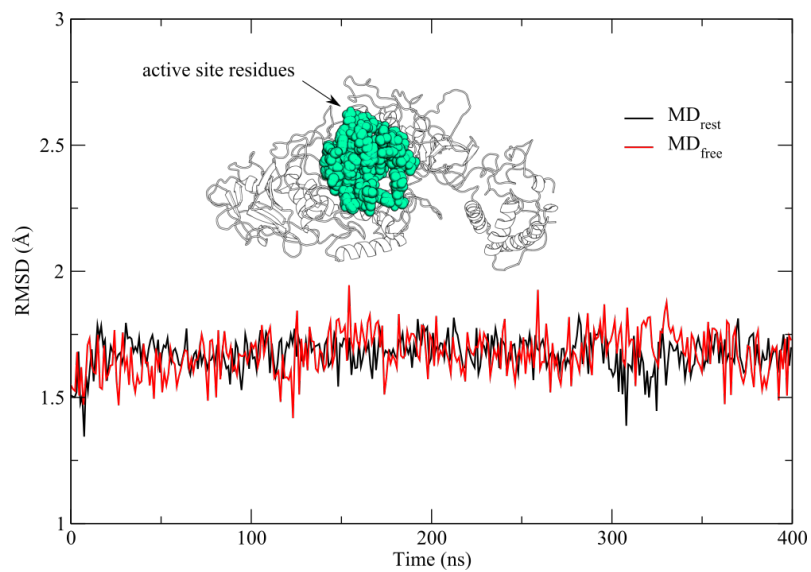


Fig. SF2 RMSD of the active site residues for the systems MD_{rest} and MD_{free} relative to the crystallographic structure with PDB ID 3AIE. t-Student test showed no significant difference between the two.

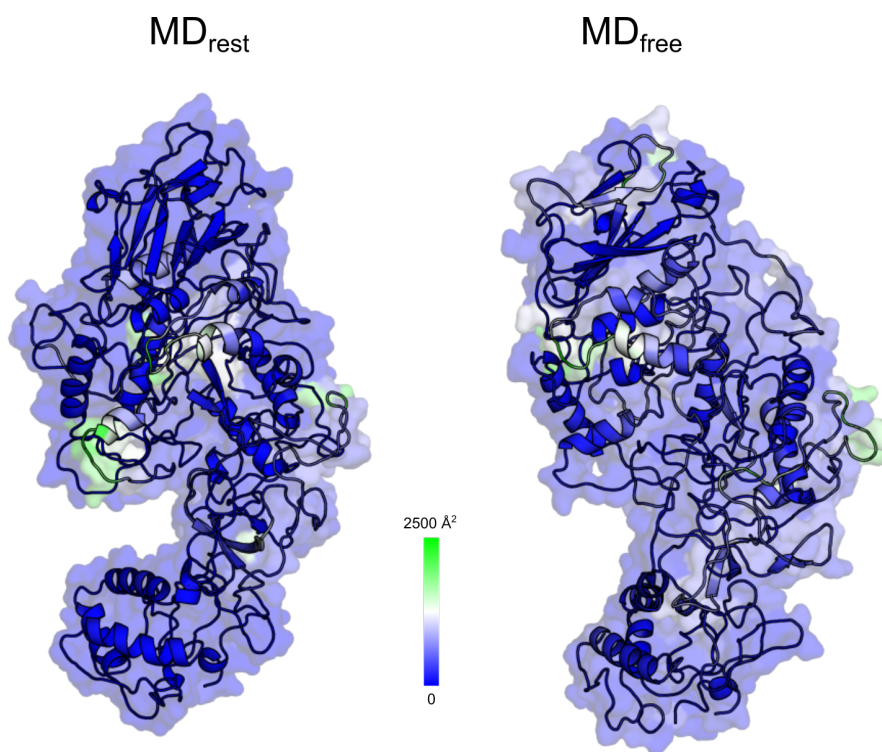


Fig. SF3 Fluctuations illustrated by B-factor on representative MD_{rest} and MD_{free} structures. Blue, white, and green colors indicate low, medium, and high residue fluctuations, respectively, calculated on the last 300 ns of the MD.

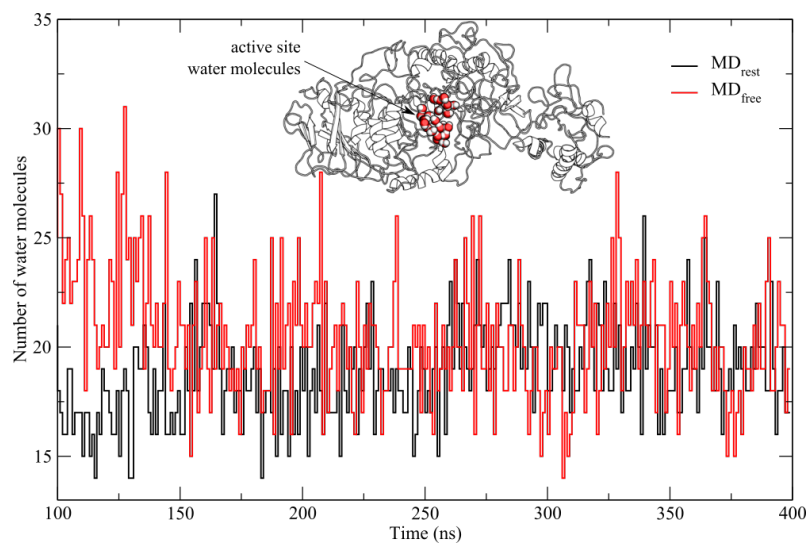


Fig. SF4 Active site water molecules present throughout the stable part of the MD production. Mean values of 19 ± 2 and 20 ± 3 water molecules for the MD_{rest} and MD_{free} systems, respectively.

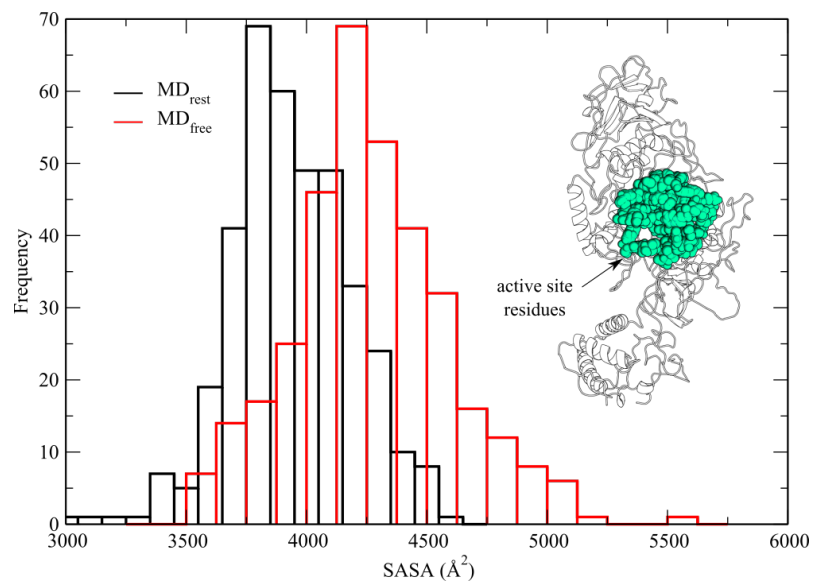


Fig. SF5 Histogram of solvent-accessible surface area for active site residues of both systems.

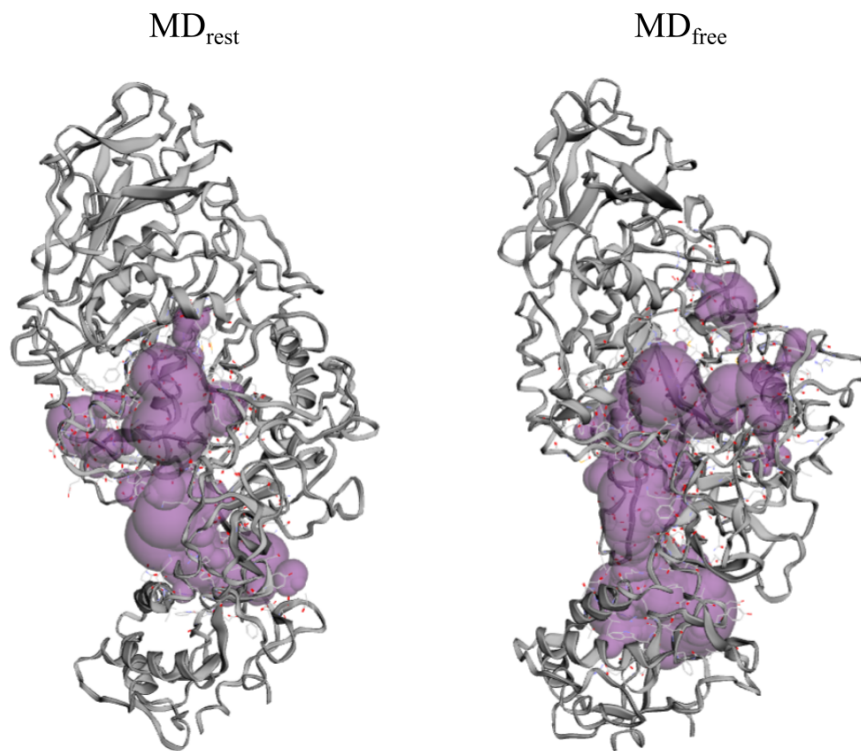


Fig. SF6 Solvent-accessible volume with values of 3518.3 and 4159.9 Å³ calculated for the inner pocket² of the MD_{rest} and MD_{free} systems, respectively.

Table ST1 Activation barriers calculated at the QM(DFTB3)/MM(CHARMM) theory level of different frames of the MD_{rest} system along the MD production and with the initial DFT-based structure.

MD _{rest} frame	E barrier, kcal·mol ⁻¹	Avg.	Std.
167	10.6		
257	13.4		
259	12.4	11.5	3.4
339	12.0		
370	5.2		
376	15.1		
DFT-based structure	6.2	-	-

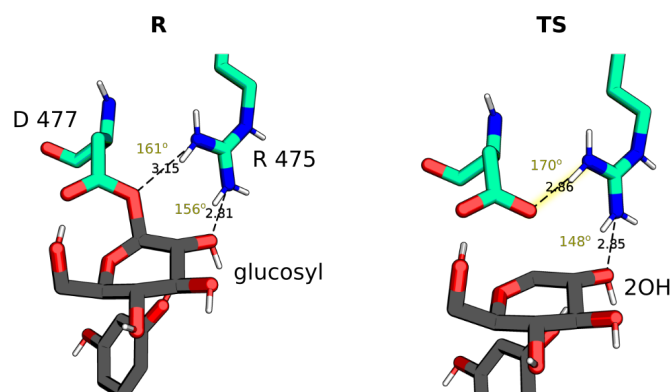


Fig. SF7 Interaction of Arg⁴⁷⁵ in the reactant and transition states of the MEP. The interaction with the 2OH group of the glucosyl moiety in the TS is highlighted due to its relevance in stabilizing the TS.

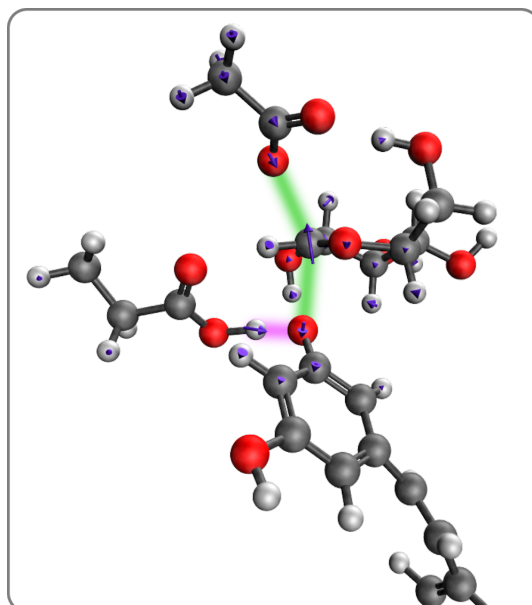


Fig. SF8 Eigenvectors (in purple) of the transition state frequency calculation. The green line shows the atoms involved in bond breaking and the nucleophilic attack. The magenta line shows the atoms involved in proton transfer.

References

- [1] Ito K, Ito S, Shimamura T, Weyand S, Kawarasaki Y, Misaka T, et al. Crystal structure of glucansucrase from the dental caries pathogen *Streptococcus mutans*. *Journal of molecular biology*. 2011;408(2):177-86.
- [2] Tian W, Chen C, Lei X, Zhao J, Liang J. CASTp 3.0: computed atlas of surface topography of proteins. *Nucleic acids research*. 2018;46(W1):W363-7.